Mass Spectrometric and Computational Studies of Heterofullerenes ($[C_{58}Pt]^-$, $[C_{59}Pt]^+$) Obtained by Laser Ablation of Electrochemically Deposited Films

Akari Hayashi,[†] Yongming Xie,[†] Josep M. Poblet,*[,‡] Josep M. Campanera,[‡] Carlito B. Lebrilla,*[,†] and Alan L. Balch*[,†]

Department of Chemistry, University of California, Davis, California 95616, and Departament de Quimica Fisica i Inorganica, Universitat Rovira i Virgili, Imperial Tarraco 1, 43005 Tarragona, Spain

Received: June 30, 2003; In Final Form: January 16, 2004

Fullerenes with metal atoms substituted into the carbon framework have been observed in laser ablation studies of electrochemically prepared C_{60}/Pt or $C_{60}/Ir(CO)_2$) films that contain polymeric, covalently bound chains: $\cdots C_{60}ML_xC_{60}ML_xC_{60}ML_x\cdots$ ($ML_x = Ir(CO)_2$ or Pt). The C_{60}/Pt film upon laser ablation produces the ions $[C_{58}Pt]^-$ and $[C_{56}Pt]^-$, which result from the substitution of a platinum atom for two carbon atoms, and $[C_{57}Pt_2]^-$, which incorporates two platinum atoms into the cage. The $C_{60}/Ir(CO)_2$ film produces a different series of products, $[C_{59}Ir]^-$, $[C_{58}Ir]^-$, $[C_{57}Ir]^-$, and $[C_{56}Ir]^-$, in which an iridium atom can replace one or two carbon atoms within the fullerene cage. Studies of the structures of $[C_{58}M]^-$ by density functional theory (DFT) show that the isomer with the metal atom replacing the C_2 unit at a 6:6 ring junction of the fullerene is more stable than the less symmetrical isomer with the metal replacing a C_2 unit at a 5:6 ring junction. Evidence for the ability of the metal atoms in some of these fullerenes to bind added ligands has been obtained by conducting the laser ablation studies in the presence of 2-butene, where adducts such as $[C_{59}Ir(2\text{-butene})]^-$, $[C_{58}Ir(2\text{-butene})]^-$, $[C_{57}Ir(2\text{-butene})]^-$, and $[C_{56}Ir(2\text{-butene})]^-$ have been observed. DFT calculations were also carried out to analyze the reactivity of $[C_{58}Pt]^-$ and $[C_{58}Ir]^-$ with ethylene as a model for 2-butene. The formation energy of $[C_{58}Ir(C_2H_4)]^-$ from $[C_{58}M]^-$ and C_2H_4 was computed to be -15.8 kcal mol^{-1}.

Introduction

Fullerenes with metal atoms bound to the outside surface are well known,[1] as are endohedral fullerenes with metal atoms confined within the interior of the fullerene cage.[2] Fullerenes with metal atoms as part of the carbon network are less common and less studied. Mass spectrometric studies have identified a number of fullerene-like clusters with heteroatoms incorporated into the carbon cage framework. Jarrold and co-workers demonstrated that $[NbC_n]^+$ clusters could be generated by the pulsed laser vaporization of graphite/NbC composites and that the mobilities of the $[NbC_n]^+$ clusters indicated that those with odd values of n contained Nb atoms that resided on the surface.[3] Related clusters can also be formed by substitution-like processes that utilize preformed fullerene cages. For example, Branz and co-workers have prepared gas-phase clusters $C_{60}M_x$ and $C_{70}M_x$ by the evaporation of the metal (M) into the fullerene vapor.[4,5] Subsequent photofragmentation of $C_{60}M_x$ and $C_{70}M_x$ produced new clusters with the compositions $C_{59-2n}M$ and $C_{69-n}M$ with M = Fe, Co, Ni, Rh, or Ir and $n = 0$, 1, or 2. As we demonstrated in our laboratories, an alternate route to the formation of the clusters, $[C_{59-2n}M]^+$ and $[C_{69-n}M]^+$,[6] involves the laser ablation of electrochemically deposited films (C_{60}/Pt or $C_{60}/Ir(CO)_2$) that contain polymeric, covalently bound chains: $\cdots C_{60}ML_xC_{60}ML_xC_{60}ML_x\cdots$ where $ML_x = Ir(CO)_2$ or Pt.[7,8] This process has been extended to form related clusters involving Sm, Ni, La, Y, and Rh.[9]

The structures of the corresponding neutral metal-substituted fullerenes have been examined in a series of computational studies. Thus, density functional theory (DFT) studies of $C_{59}Pt$ and $C_{59}Ir$ have shown that the metal atoms are found in three coordinate sites on the fullerene surface.[4] Because the Ir−C or Pt−C bonds are longer than C−C bonds, the Ir or Pt atoms protrude outward on the fullerene surface, and the theoretical work indicated that the addition of a ligand to the exposed metal atom would be energetically favorable. Studies of $C_{59}Fe$ revealed a similar structure.[10] Computational studies of the structures of $C_{69}M$, where M = Co, Rh, and Ir, showed that substitution at sites at the more highly pyramidalized poles of the fullerene was energetically favored.[11]

Here we report the observation of new heterofullerenes with metal atoms incorporated into the fullerene network through the replacement of two carbon atoms by a single metal atom and present experimental evidence for the ability of $[C_{59}M]^+$ and $[C_{58}M]^-$ to bind to olefins. The structures of $C_{58}M$ and related species have been studied by DFT calculations.

Results and Discussion

Laser Ablation Studies of C_{60}/Pt and $C_{60}/Ir(CO)_2$ Films. Previous work that examined the products in the positive ion mode revealed that the ions $[C_{59}Ir]^+$ and $[C_{59}Pt]^+$ are formed during the laser ablation process from (η^2-C_{60})Pt or (η^2-C_{60})-$Ir(CO)_2$ units that are present in the electrochemically deposited films.[6] As reported earlier, no evidence for the existence of the corresponding substitution products, $[C_{59}Pt]^-$ or $[C_{59}Ir]^-$, was seen in the negative ion mode mass spectra. The spectra from either film in the negative ion mode revealed only the features due to $[C_{60}]^-$ and its fragmentation products.

However, further studies of these films have revealed that the negative ion spectra are strongly dependent on the intensity

* Corresponding authors. E-mail: albalch@ucdavis.edu.
[†] University of California.
[‡] Universitat Rovira i Virgili.

10.1021/jp035876h CCC: $27.50
Published on Web 03/02/2004

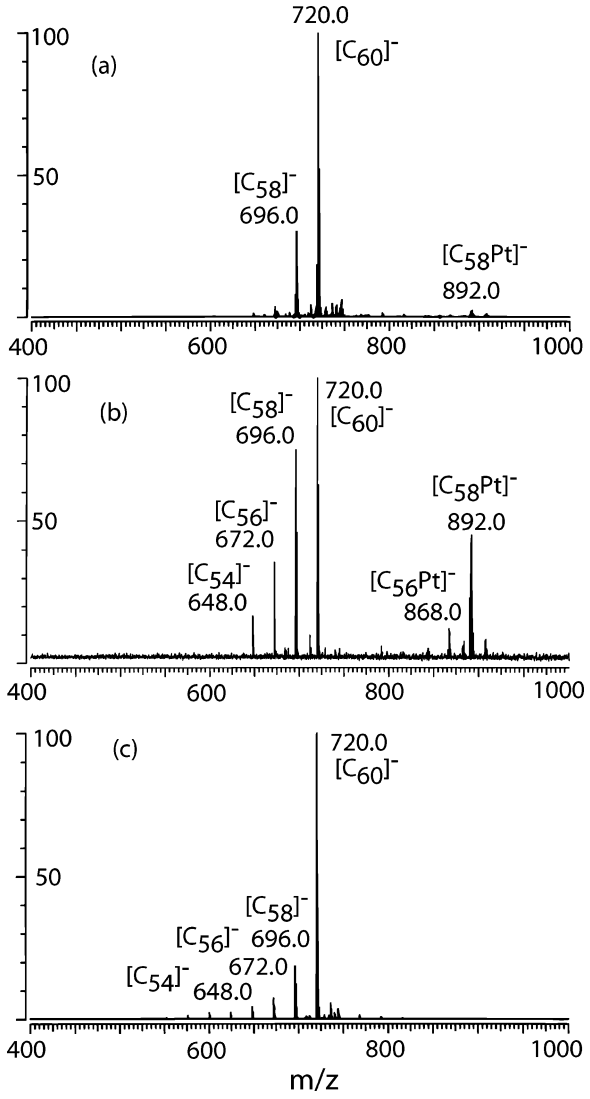

Figure 1. Mass spectra (negative-ion mode) obtained by laser ablation of a electrochemically deposited C_{60}/Pt film with three different values of the qualitatively increasing laser intensity: (a) 5, (b) 7.5, and (c) 15.

of the laser beam, as shown in Figure 1 from data obtained from a C_{60}/Pt film. As seen in trace b of Figure 1, it is possible to detect a cluster of peaks at 892 amu due to $[C_{58}Pt]^-$ along with a set of peaks due to $[C_{56}Pt]^-$, which may be formed from $[C_{58}Pt]^-$ by the usual loss of a C_2 fragment. The data in trace b were obtained with a laser power greater than that available to us in the previous work. Additionally, at all laser powers the spectrum of $[C_{60}]^-$ is seen, and peaks due to the ions $[C_{60-2n}]^-$ that result from C_2 loss are also observed with varying intensities.

Figure 2 shows an expansion of the high-mass region observed during laser ablation of the C_{60}/Pt film. In this region, there are prominent features due to $[C_{58}Pt]^-$ and its fragmentation product $[C_{56}Pt]^-$, along with peaks due to $[C_{58}PtO]^-$ and its fragmentation product $[C_{56}PtO]^-$. The oxygen atoms in the latter two species are believed to reside in epoxide-like units on the fullerene surface and to arise from the oxidation of the fullerene film during air exposure. It is known that fullerenes are susceptible to facile atmospheric oxidation,[12] and the film was exposed to air during the transfer from the electrochemical cell in which it was prepared to the mass spectrometer. A small peak due to $[C_{60}PtCl]^-$ is also observed. The chlorine in this ion may result from chloride ion from the film precursor, $\{Pt(\mu\text{-}Cl)Cl(C_2H_4)\}_2$, or from residual amounts of the supporting electrolyte, tetra(*n*-butyl)ammonium perchlorate, present in the C_{60}/Pt film. A cluster of peaks at 1062 amu is due to $[C_{56}Pt_2]^-$. A comparison of the observed and calculated patterns of masses of $[C_{56}Pt_2]^-$ resulting from the naturally occurring isotopes of C and Pt is shown in the insets to Figure 2. Another cluster of peaks at 1078 amu has been found to result from the presence of two other species, $[C_{57}Pt_2]^-$ and $[C_{56}Pt_2O]^-$.[13] Again, the insets show the experimental data along with the computed spectral patterns for $[C_{57}Pt_2]^-$ and $[C_{56}Pt_2O]^-$.

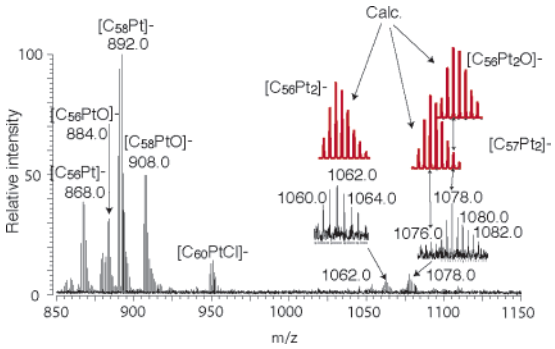

Figure 2. Mass spectrum (negative-ion mode) obtained by laser ablation of the electrochemically deposited C_{60}/Pt film after the ejection of the $[C_{60}]^-$ ion. The insets show expansions of the multiplets observed for $[C_{56}Pt_2]^-$, $[C_{57}Pt_2]^-$, and $[C_{56}Pt_2O]^-$ and comparisons with the calculated spectra.

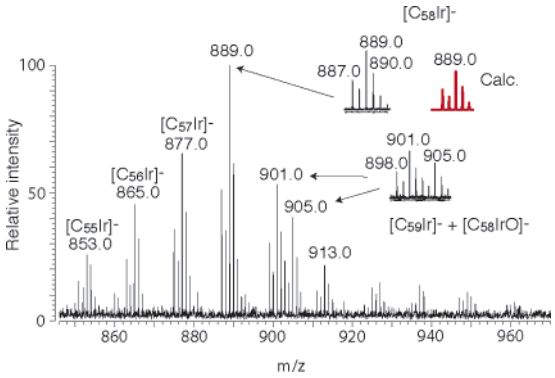

Figure 3. Mass spectrum (negative-ion mode) obtained by laser ablation of the electrochemically deposited $C_{60}/Ir(CO)_2$ film after the exclusion of the $[C_{60}]^-$ ion. The insets show expansions of the multiplets observed for $[C_{58}Ir]^-$, $[C_{59}Ir]^-$, and $[C_{58}IrO]^-$ and comparisons with the calculated spectrum.

Figure 3 shows a similar expansion of the high-mass region observed during laser ablation of the $C_{60}/Ir(CO)_2$ film. A number of new anions are observed. Most prominent of these is $[C_{58}Ir]^-$ with a cluster at 889 amu. The insets compare the experimental and calculated patterns of the spectrum for this species. An overlapping set of peaks in the 898−907 region has been identified as originating from $[C_{59}Ir]^-$ and $[C_{58}IrO]^-$. Other features in the spectrum are identified with ions $[C_{57}Ir]^-$, $[C_{56}Ir]^-$, and $[C_{55}Ir]^-$. Ions $[C_{57}Ir]^-$ and $[C_{55}Ir]^-$ are obtained possibly from $[C_{59}Ir]^-$ by successive losses of C_2 units, and $[C_{56}Ir]^-$ may be obtained from $[C_{58}Ir]^-$ by a similar C_2 loss.

There is evidence that ions $[C_{60}M_n]^+$ and $[C_{70}M_n]^+$ with metal atoms coating the outside of intact C_{60} and C_{70} molecules exist in the gas phase.[4,5] However, we did not detect significant quantities of any the hypothetical ions $[C_{60}Pt_n]^-$ or $[C_{60}Ir_n]^-$ in our experiments. Rather, what we have found are species that appear from their composition to involve the substitution of carbon atoms by platinum or iridium. To examine the structure of such heterofullerenes, we have performed DFT calculations.

TABLE 1: Substitution Energy, Cage Radius, Bond Lengths, Mulliken Net Charges, and Spin Densities for Several Fullerenes with Metal Atoms within the Carbon Framework[a]

molecule	substitution energy[b]	cage radius[c]	M−C bond lengths	Mulliken net charge		spin density	
				M	C[d]	M	C[d]
$C_{59}Pt$	5.24	3.579	1.980/1.925	0.618	−0.355		
$C_{58}Pt$ (C_{2v})	6.57	3.561	2.016	0.619	−0.379		
$C_{58}Pt$ (C_s)	7.15	3.569	2.031/1.992	0.610	−0.367		
$C_{58}Ir$ (C_{2v})	5.32	3.558	2.033	0.955	−0.396	0.441	0.066
$C_{58}Ir$ (C_s)	5.93	3.562	2.055/1.988	0.959	−0.394	0.443	0.074
$[C_{58}Pt\ (C_{2v})]^-$		3.564	2.018	0.579	−0.401	0.204	0.036
$[C_{58}Pt\ (C_{2v})]^+$		3.558	2.025	0.660	−0.343	0.279	0.074
$[C_{58}Ir\ (C_{2v})]^-$		3.561	2.023	0.933	−0.442		

[a] Energies in eV and distances in Å. [b] Energy corresponding to the process $C_{60} + M \rightarrow C_{59}M + C$ for $C_{59}M$ and to the process $C_{60} + M \rightarrow C_{58}M + C_2$ for $C_{58}M$. [c] Cage radius is defined as the average distance of all surface atoms to the center of the fullerene. Cage radius for C_{60} is 3.549 Å. [d] Average values for the carbon atoms bonded to the metal.

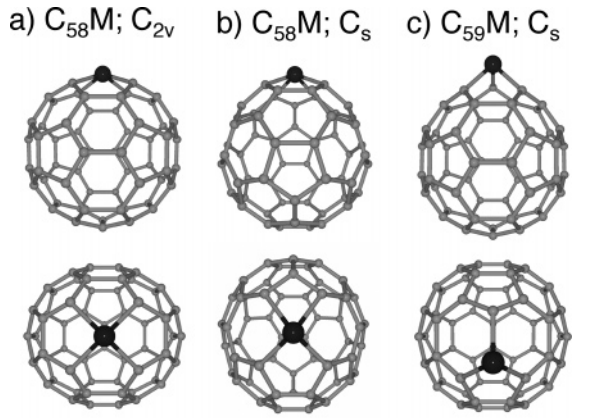

Figure 4. Two orthogonal views of the calculated structures of (a) the C_{2v} isomer of $C_{58}M$ (6:6 C−C bond substitution), (b) the C_s isomer of $C_{58}M$ (6:5 substitution), and (c) $C_{59}M$.

Figure 5. Three-dimensional representations of the HOMO (with symmetry B_1) and the LUMO (with symmetry B_2) for the most stable (C_{2v}) isomer of $C_{58}M$. For clarity, two perpendicular views are given for the LUMO.

DFT Studies of the Structure of $C_{58}M$. The geometries of these heterofullerenes have been computed by DFT. Drawings of the computed structures of $C_{58}M$ are shown in Figure 4, where they are compared with the previously computed structure of $C_{59}M$.[6] The substitution of a metal atom for a C_2 unit in C_{60} results in the formation of two different isomers because the C_2 unit can be removed from a 6:6 ring junction to produce an isomer with C_{2v} symmetry or a 6:5 ring junction to produce the lower-symmetry C_s isomer. Table 1 contains selected distances for the two isomers of $C_{58}Pt$ and $C_{58}Ir$. As seen in Figure 4, the four-coordinate metal atoms in both isomers of $C_{58}M$ do not protrude very far away from the fullerene surface. In contrast, the three-coordinate metal atom in $C_{59}M$ bulges away from the fullerene surface as seen in Figure 4c.

In the C_{2v} isomer, the deformation of the C_{58} core is very small and is restricted to the carbons directly linked to the metal. In the C_s isomer, the deformation of the carbon cage is somewhat greater. For both $C_{58}Pt$ and $C_{58}Ir$, the C_{2v} isomer is more stable than the C_s isomer. The energy differences between these two structures are 0.58 eV for Pt and 0.61 eV for Ir, as seen in Table 1.

The substitution of a 6:6 C_2 unit in C_{60} by a metal atom is a process that requires considerable energy when the metal is a platinum atom (6.57 eV) and a slightly lower energy when the heteroatom is an iridium atom (5.32 eV). In general in the iridium compounds, the metal−carbon bond lengths are slightly longer; consequently, the metal is pulled away slightly from the cage surface, an effect that increases the cage radius in relation to that of the platinum derivative. Semiempirical studies on B and N heterofullerenes of C_{60}[14] and C_{70}[15] and DFT calculations on $C_{59}M$[16] (M = Fe, Co, Ni, and Rh) also showed that the doped fullerenes are less stable than their all-carbon analogues.

The ground state for the most stable isomer of $C_{58}Pt$ is a singlet with a relatively large HOMO−LUMO gap of 0.59 eV. The triplet state is 11.5 kcal mol^{-1} above the ground state. Mulliken population analysis indicates that there is charge transfer from the metal to the carbon cage in $C_{58}Pt$. The net charge on the metal center is +0.619e, and the negative charge on the carbon atoms bonded to platinum is −0.379e. The rest of the carbon atoms exhibit smaller charges. The electronic populations of the s, p, and d Pt orbitals are 2.915e, 6.174e, and 8.293e, respectively. These values are similar to the electronic populations of the corresponding orbitals in $C_{59}Pt$ (2.801e, 6.206e, and 8.376e).[17] The Voronoi partition scheme of the electron density suggests that the transfer of charge is greater because this method gives a net charge of +1.444e for the metal center and −0.415e for the carbon atoms connected to Pt.

As in $C_{59}Pt$,[6] the highest occupied orbitals in $C_{58}Pt$ and $C_{58}Ir$ are formally metal d orbitals. However, in the substituted transition metal−fullerene compounds, the d-metal orbitals are spread through several molecular orbitals. Specifically, the contribution of the platinum d orbitals in $C_{58}Pt$ is 21% in the HOMO, 12% in the HOMO-1, and 13% in the LUMO. Three-dimensional representations of these orbitals are shown in Figure 5. Spin densities computed for the oxidized and reduced partners confirm that the platinum d orbitals are spread through many different molecular orbitals. Hence, for the anion $[C_{58}Pt]^-$, the spin density is delocalized over the carbon skeleton with only 0.20e localized on Pt, whereas in $[C_{58}Pt]^+$ 0.28e is localized on the metal center. Jinlong and co-workers reported similar electronic properties in C_{60}- and C_{70}-doped fullerenes ($C_{59}M$, with M = Fe, Co, Ni, and Rh; $C_{69}M$, with M = Co, Rh, and Ir).[16]

TABLE 2: Physical Properties of C_{60} and Several Pt- and Ir-Substituted Fullerenes[a]

	C_{60}	$C_{58}Pt^c$	$C_{58}Ir^c$	$C_{59}Pt^b$	$C_{59}Ir^b$
IP	7.51	7.28	6.97	7.39	7.10
EA	2.85	3.69	3.60	3.56	3.71
E(LUMO)[d]	−4.59	−5.47	−5.32	−5.34	−5.08
E(HOMO)[d]	−6.24	−6.06	−5.65	−6.05	−5.64

[a] Values in eV. [b] Reference 6. [c] Isomer C_{2v}. [d] Energies for the HOMO and LUMO correspond to the energies of the α singly occupied orbital and its β unoccupied counterpart, respectively.

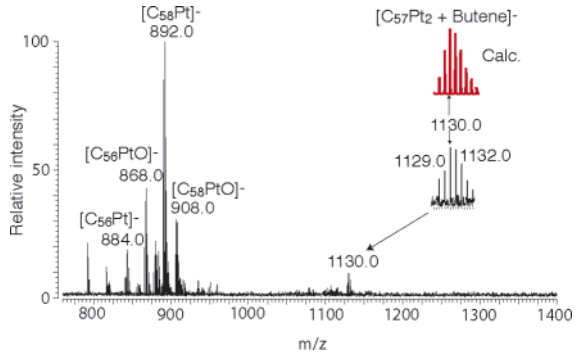

Figure 6. Mass spectrum (negative-ion mode) obtained by laser ablation of the C_{60}/Pt film in a butene atmosphere. The $[C_{60}]^-$ ion was ejected from the ICR cell after the ions formed in the cell were collided with butene gas. The inset shows an expansion of the multiplet observed for $[C_{57}Pt_2(2\text{-butene})]^-$ and a comparison with the calculated spectrum.

The ground state of the analogous iridium complex, $C_{58}Ir$, is a doublet of symmetry B_1 in which the spin density is 0.441e on the metal center and 0.066e on each of the adjacent carbon atoms. The remaining spin density is delocalized thoughout the carbon cage. The net charges of +0.955e on Ir and −0.396e on its neighboring carbon atoms indicate that charge transfer is slightly more important in $C_{58}Ir$ than in $C_{58}Pt$. Voronoi charges confirm this trend and give a net charge of +1.554e for the iridium atom. For more details about net charges and spin densities, see Table 1.

Selected physical properties for the heterosubstituted fullerenes and for C_{60} are given in Table 2. At the present level of theory, the electron affinities (EA) for $C_{58}Pt$ and $C_{58}Ir$ are calculated to be 3.69 and 3.60 eV, respectively, which are slightly higher than the EA of C_{60}, 2.85 eV. Smalley and co-workers estimated an EA of ca. 2.60−2.80 eV for C_{60} from its photoelectron spectrum.[18] The computed ionization potentials (IP), 7.28 eV for $C_{58}Pt$ and 6.97 eV for $C_{58}Ir$, suggest that these heterofullerenes lose electrons somewhat more readily to form positive ions than does C_{60}. The calculated and the experimental IPs for C_{60} are 7.51 and 7.6 eV, respectively.[19] The changes in the EAs and IPs are easily understood from the relative energies of the HOMO and LUMO. Hence, these new heterofullerenes have somewhat smaller ionization potentials and greater electron affinities than those of C_{60}. This trend was found for Si-,[20] N-, and B-substituted fullerenes[14] and metal heterofullerenes such as $C_{59}M$ (M = Pt, Ir, Fe, Co, Ni, and Rh).[16]

Reactions of $[C_{60-n}Pt]^-$ and $[C_{60-n}Ir]^-$ with 2-Butene. To demonstrate that the metal atoms in these newly formed clusters were indeed on the outside of the fullerene where they were exposed to added substrates, we investigated the reactions of these new cluster ions with a potential ligand, 2-butene. Prior DFT calculations indicated that such ligand additions should occur with $C_{59}M$.[6]

Figure 6 shows the results of a similar experiment with laser ablation of a C_{60}/Pt film in the presence of 2-butene. In this case, a comparison with the data shown in Figure 2 reveals the presence of only one new species, $[C_{57}Pt_2(2\text{-butene})]^-$. The ions $[C_{58}Pt]^-$, $[C_{56}Pt]^-$, $[C_{58}PtO]^-$, and $[C_{56}PtO]^-$ appear to be unreactive toward the binding of 2-butene under these conditions.

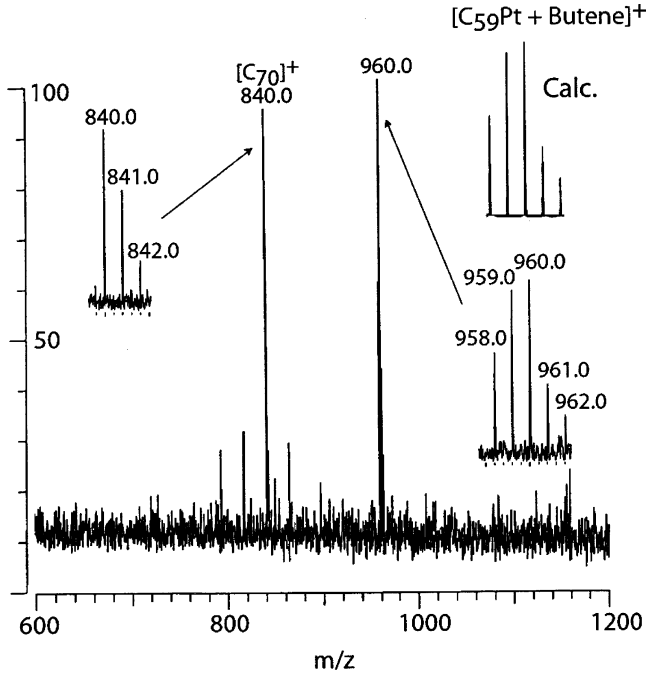

Figure 7. Mass spectrum (positive-ion mode) obtained by laser ablation of the C_{60}/Pt film in a butene atmosphere. The $[C_{60}]^+$ ion was ejected from the ICR cell after the ions formed in the cell were collided with butene gas. The spectrum shows an expansion of the multiplet observed for $[C_{59}Pt(2\text{-butene})]^+$ and a comparison with the calculated spectrum.

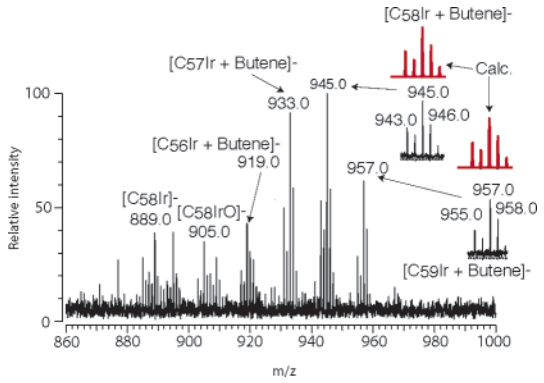

Figure 8. Mass spectrum (negative-ion mode) obtained by laser ablation of a $C_{60}/Ir(CO)_2$ film in a butene atmosphere. The $[C_{60}]^-$ ion was ejected from the ICR cell after the molecules formed in the cell were collided with butene gas. The insets show expansions of the multiplets observed for $[C_{59}Ir(2\text{-butene})]^-$ and $[C_{58}Ir(2\text{-butene})]^-$ and comparisons with the calculated spectra.

In view of the low reactivity of $[C_{58}Pt]^-$ and $[C_{56}Pt]^-$ toward 2-butene, the reactivity of $[C_{59}Pt]^+$ toward addition was also examined. As shown in Figure 7, $[C_{59}Pt]^+$ does add 2-butene to form $[C_{59}Pt(2\text{-butene})]^+$.

Figure 8 shows the high-mass portion of the spectrum acquired upon laser ablation of a $C_{60}/Ir(CO)_2$ film in an atmosphere of 2-butene. Comparison with Figure 3 reveals the formation of several new species, including $[C_{59}Ir(2\text{-butene})]^-$, $[C_{58}Ir(2\text{-butene})]^-$, $[C_{57}Ir(2\text{-butene})]^-$, and $[C_{56}Ir(2\text{-butene})]^-$. Clearly, the metal ions in $[C_{60-n}Ir]^-$ with both odd and even n can add an external ligand. As seen in Figure 6, small amounts of $[C_{58}Ir]^-$ and $[C_{58}IrO]^-$ remain, but these species have lower abundances than do the 2-butene-containing ions. It is particu-

Figure 9. Computed structure for the $[C_{58}Ir(C_2H_4)]^-$ adduct.

TABLE 3: Selected Distances Calculated for Several Fullerene Adducts[a]

molecule	cage radius	M−C (fullerene)	M−C (ethylene)	C−C (ethylene)
$[C_{58}Ir(C_2H_4)]$	3.556	2.039	2.479	1.373
$[C_{58}Ir(C_2H_4)]^-$	3.559	2.038	2.236	1.425
$[C_{58}Pt(C_2H_4)]$	3.557	2.009	2.447	1.373
$[C_{58}Pt(C_2H_4)]^-$	3.560	2.012	2.435	1.375

[a] Values in Å.

larly interesting that both $[C_{58}Ir]^-$ and $[C_{56}Ir]^-$ bind 2-butene whereas $[C_{58}Pt]^-$ and $[C_{56}Pt]^-$ are unreactive under similar conditions.

DFT Studies of the Interaction of Ethylene with Heteroatom-Substituted Fullerenes. DFT calculations were also carried out to analyze the reactivity of $[C_{58}Pt]^-$ and $[C_{58}Ir]^-$ with 2-butene. To simplify the problem and to save computer time, the 2-butene ligand was modeled as an ethylene molecule. The computed structure of $[C_{58}Ir(C_2H_4)]^-$ is shown in Figure 9, and Table 3 contains selected distances in these adducts. The ethylene ligand coordinates to the metal in the $C_{58}M$ clusters without altering the structure of the fullerene, as the values in Table 3 show.

The process

$$C_{58}M + C_2H_4 \rightarrow C_{58}M(C_2H_4) \quad (M = Pt \text{ or } Ir)$$

is exothermic for both neutral and monoanionic molecules. The formation energy of $[C_{58}Ir(C_2H_4)]^-$ from $[C_{58}M]^-$ and C_2H_4 units was computed to be -15.8 kcal mol^{-1}. This relatively large value is consistent with the experimental observation of a peak in the mass spectrum that may be associated with $[C_{58}Ir(2\text{-butene})]^-$. This adduct is computed to have a metal−ligand distance of 2.236 Å, one that is only slightly larger than that found in conventional organometallic iridium complexes in which the Ir−C bond lengths range from 2.03 to 2.21 Å.[21] The energy involved in the formation of the analogous complex of platinum, $[C_{58}Pt(C_2H_4)]^-$, is -12.4 kcal mol^{-1}. Although $[C_{58}Pt(2\text{-butene})]^-$ was not observed in the laser ablation experiment from a C_{60}/Pt film in the presence of 2-butene, our DFT calculations indicate that $C_{58}Pt$ may coordinate olefins through the platinum atom. The reactivity of $C_{59}M$ with CO has also been explored through DFT calculations, and the addition of CO to the platinum atom is possible.[6]

To characterize the heterofullerene−ethylene bond, we performed a decomposition of the interaction energy between both fragments through an extension of the Morokuma decomposition scheme[22] as developed by Ziegler and Rouk.[23] According to this scheme, the bonding energy (BE) between the fullerene and ethylene can be decomposed into three main contributions:

$$BE = \Delta E_{DE} + \Delta E_{ST} + \Delta E_{ORB}$$

The deformation energy (ΔE_{DE}) is the energy necessary to convert both fragments from their equilibrium geometries to the geometries found in the cluster. The steric interaction term (ΔE_{ST}) represents the interaction energy between the two deformed fragments with the electron densities that each fragment would have in the absence of the other fragments. This term can be decomposed into an exchange repulsion or Pauli repulsion term (ΔE_{Pauli}) and an electrostatic term (ΔE_{elstat}). Finally, the orbital interaction term (ΔE_{ORB}) includes the stabilization produced when the unperturbed fragment electron densities are allowed to relax and can be decomposed into ΔE_{A1}, ΔE_{A2}, ΔE_{B1}, and ΔE_{B2} according to the irreducible representations of the C_{2v} symmetry group. This method has recently been used to rationalize the bonding between guest and host in the endohedral $Sc_3N@C_{78}$ and $Sc_3N@C_{80}$ clusters[24] and the metal−fullerene bond in the $(\eta^2\text{-}C_{60})M(PH_3)_2$ (M = Ni, Pd, and Pt) complexes.[25]

The different terms for the bonding-energy partition in the neutral and anionic complexes $[C_{58}M(C_2H_4)]$ (M = Ir and Pt) are given in Table 4. For $[C_{58}Ir(C_2H_4)]$, the deformation energy is only 4.3 kcal mol^{-1} because the alteration of both the cage and the ethylene units with respect to the isolated molecules is very small. The Pauli repulsion (109.8 kcal mol^{-1}) is larger than the electrostatic term (-73.7 kcal mol^{-1}); therefore, the steric term that is the sum of these two contributions is repulsive ($+36.1$ kcal mol^{-1}). The orbital term, which amounts to -49.6 kcal mol^{-1}, overcomes the repulsive steric term and the deformation energy of the fragments. Thus, the orbital term is responsible for adduct formation. An examination of the ΔE_{ORB} values (Table 4) shows that the A_1 orbital interactions, which produce the σ donation from the π ethylene orbital to the metal orbitals, clearly make the largest contribution (-30.2 kcal mol^{-1}) to ΔE_{ORB} and therefore to the total binding energy. The contribution associated with the B_1 orbitals, which accounts for the π back-donation, is only -16.2 kcal mol^{-1}. The other orbital contributions are almost negligible. In contrast, when the fullerene acts as a ligand in complexes such as $(\eta^2\text{-}C_{60})M(PH_3)_2$ (M = Ni, Pd, and Pt), Sgamelloti and co-workers have demonstrated that the π back-donation from the metal to the fullerene is more important than the corresponding ligand-to-metal σ donation.[25]

The addition of one electron to the singly occupied bonding orbital of B_1 symmetry in $[C_{58}Ir(C_2H_4)]$ shortens the M−ethylene bond length from 2.479 Å in the neutral complex to 2.236 Å in the reduced partner. This shortening is accompanied by a larger deformation of the ethylene fragment, and the ΔE_{DE} term increases to 15.0 kcal mol^{-1}. The repulsive ΔE_{ST} and the attractive ΔE_{ORB} terms also become larger after reduction, and the total Ir−ethylene bonding energy is greater by 6.6 kcal mol^{-1} when the π back-donation orbital represented in Figure 10 accommodates two electrons. Notice from the data in Table 4 that in the anionic $[C_{58}Ir(C_2H_4)]^-$ complex the contribution of the B_1 orbitals to the ΔE_{ORB} term is larger than the electron density rearrangement associated with the mixing between A_1 orbitals. This observation suggests that in $[C_{58}Ir(C_2H_4)]^-$ π back-donation is more important than the σ donation.

As expected from the isoelectronic nature of $[C_{58}Pt(C_2H_4)]$ and $[C_{58}Ir(C_2H_4)]^-$, these two complexes have similar binding energies (Table 4). However, in the platinum complex, ethylene coordinates the transition-metal atom at quite a long distance, 2.447 Å, a bond length that is similar to the corresponding value computed for the neutral iridium complex. Usually, the Pt(0)−ethylene bond length is close to 2.10 Å,[26] and many theoretical studies have shown that the Pt(0)−ethylene bond in $(\eta^2\text{-}CH_2{=}CH_2)Pt(PH_3)_2$ is stronger, with dissociation energies between 20 and 28 kcal mol^{-1}.[27] Therefore, one can conclude from the

TABLE 4: Decomposition of the Binding Energy (kcal mol^{-1}) for Several [$C_{58}M(C_2H_4)$] Adducts[a]

		$[C_{58}Ir(C_2H_4)]$	$[C_{58}Ir(C_2H_4)]^-$	$[C_{58}Pt(C_2H_4)]$	$[C_{58}Pt(C_2H_4)]^-$
ΔE_{DE}	cage	2.7	5.8	3.1	3.6
	ethylene	1.6	9.2	1.6	1.7
	total	4.3	15.0	4.7	5.3
ΔE_{ST}	ΔE_{Pauli}	109.8	226.8	108.9	119.3
	ΔE_{elstat}	−73.7	−153.6	−73.8	−79.1
	total	36.1	73.2	35.1	40.2
ΔE_{ORB}	$\Delta E_{A1}(\sigma)$	−30.3	−45.1	−36.5	−34.5
	ΔE_{A2}	−0.7	−0.9	−0.6	−0.4
	$\Delta E_{B1}(\pi)$	−16.2	−53.5	−16.9	−20.3
	ΔE_{B2}	−2.4	−4.5	−2.0	−2.7
	total	−49.6	−104.0	−56.0	−57.9
BE[a]		−9.2	−15.8	−16.2	−12.4

[a] The binding energy is the energy difference between the optimized (C_{2v}) [$C_{58}M(C_2H_4)$] adduct and the two relaxed $C_{58}M$ and C_2H_4 fragments.

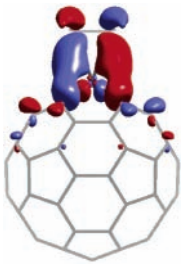

Figure 10. Three-dimensional representation of the π back-donation orbital for $[C_{58}Ir(C_2H_4)]^-$.

present studies that π-bonding ligands might coordinate to C_{58}-Pt but with an interaction that is weaker than that in the corresponding phosphine complexes. The partitioning energy values for $[C_{58}Pt(C_2H_4)]$ indicate that the orbital term is clearly dominated by σ donation as it is in the neutral Ir complex. In other words, the ligand → metal σ donation is more effective than the metal → ligand π back-donation for long M−ethylene bonds. For an extensive discussion of the nature of bonding in transition-metal complexes, see the recent review by Frenking and Frölich.[28]

The reduction of the neutral platinum complex to give $[C_{58}Pt(C_2H_4)]^-$ differs from the corresponding reduction of the iridium complex because the added electron goes into an orbital of B_2 symmetry that has nonbonding character between the heterofullerene and the ethylene ligand. Consequently, the orbital interaction and the deformation energy of both fragments are not modified significantly. The C−C bond in ethylene remains almost invariant, whereas the Pt−ethylene bond length increases only slightly, 0.012 Å. The smaller binding energy for the anionic $[C_{58}Pt(C_2H_4)]^-$ cluster (108.9 kcal mol^{-1} in the neutral complex, 119.3 kcal mol^{-1} in the anion) can be attributed to an increase in Pauli repulsion between ethylene and the negatively charged heterofullerenes.

Experimental Section

Materials. The C_{60}/Pt and C_{60}/Ir(CO)$_2$ films were prepared electrochemically from toluene/acetonitrile (4:1 v/v) solutions of C_{60} (0.35 mM) and $\{Pt(\mu\text{-Cl})Cl(C_2H_4)\}_2$ (0.80 mM) or Ir(CO)$_2$Cl(p-toluidine) (0.85 mM), respectively, with 0.1 M tetra(*n*-butyl)ammonium perchlorate as the supporting electrolyte, as reported previously.[7,8] For a working electrode, a Pt or Ir foil (0.3 × 0.5 cm^2) was used. After the formation of each film, the film-covered Pt or Ir foil was washed several times with a fresh toluene/acetonitrile (4:1 v/v) solution. The film was dried in air and transferred to the mass spectrometer.

Instrumentation. Mass spectra were recorded on a matrix-assisted laser desorption/ionization Fourier-transform mass spectrometer (HiRes MALDI, Ion Spec Corporation, Irvine, CA) with a 4.7-T magnet and a nitrogen laser emitting at 337 nm. The electrochemically prepared films were place on the probe tip without any matrix.

Theoretical Details. The calculations were carried out using DFT methodology with the ADF2000 program.[29] The local density approximation (LDA) characterized by the electron gas exchange and with the Vosko−Wilk−Nusair[30] (VWN) parametrization for correlation were used. Gradients were corrected by means of the Becke[31] and Perdew[32] nonlocal corrections to the exchange and correlation energy, respectively. Triple-ζ plus polarization Slater basis sets were used to describe the valence electrons of carbon atoms. For platinum and iridium atoms, the inner electrons 1s−4spd were considered to be frozen and were described by means of single Slater functions; the 5s and 5p electrons, by double-ζ Slater functions; the 5d and 6s electrons, by triple-ζ functions; and the 6p electrons, by a single orbital.[33] The Pauli formalism with corrected core potentials was used to make quasi-relativistic corrections for the core electrons. The quasi-relativistic frozen-core shells were generated using the auxiliary program DIRAC.[27] Open-shell electronic configurations were computed with the unrestricted methodology.

Acknowledgment. We thank the National Science Foundation (grants CHE 0070291 to A.L.B. and CHE 9982166 to C.B.L.) for financial support and Johnson Matthey for the loan of platinum and iridium salts. DFT calculations have been carried out on workstations purchased with funds provided by the DGICYT of the Government of Spain and by the CIRIT of Generalitat of Catalunya (grant nos. BQU2002-04110-C02-02 and SGR01-00315).

References and Notes

(1) Balch, A. L.; Olmstead, M. M. *Chem. Rev.* **1998**, *98*, 2123.

(2) Shinohara, H. In *Fullerenes: Chemistry, Physics and Technology*; Kadish, K. M., Ruoff, R., Eds.; Wiley and Sons: New York, 2000; p 357.

(3) Clemmer, D. E.; Hunter, J. M.; Shelimov, K. B.; Jarrold, M. F. *Nature* **1994**, *372*, 248.

(4) Branz, W.; Billas, I. M. L.; Malinowski, N.; Tast, F.; Heinebrodt, M.; Martin, T. P. *J. Chem. Phys.* **1998**, *109*, 3425.

(5) Billas, I. M. L.; Branz, W.; Malinowski, N.; Tast, F.; Heinebrodt, M.; Martin, T. P.; Massobrio, C.; Boero, M.; Parrinello, M. *Nanostruct. Mater.* **1999**, *12*, 1071.

(6) Poblet, J. M.; Winkler, K.; Cancilla, M.; Hayashi, A.; Lebrilla, C. B.; Balch, A. L. *Chem. Comm.* **1999**, 493.

(7) Balch, A. L.; Costa, D. A.; Winkler, K. *J. Am. Chem. Soc.* **1998**, *120*, 9614.

(8) Hayashi, A.; de Bettencourt-Dias, A.; Winkler, K.; Balch, A. L. *J. Mater. Chem.* **2002**, *12*, 2116.

(9) Kong, Q.; Shen, Y.; Zhao, L.; Zhuang, J.; Qian, S.; Li, Y.; Lin, Y.; Cai, R. *J. Chem. Phys.* **2002**, *116*, 128.

(10) Billas, I. M. L.; Massobrio, C.; Boero, M.; Parrinello, M.; Branz, W.; Tast, F.; Malinowski, N.; Heinebrodt, M.; Martin, T. P. *Comput. Mater. Sci.* **2000**, *17*, 191.

(11) Changgeng, D.; Jinlong, Y.; Rongsheng, H.; Kelin, W. *Phys. Rev. A* **2001**, *64*, 43201.

(12) Taylor, R.; Barrow, M. P.; Drewello, T. *Chem. Commun.* **1998**, 2497.

(13) When two metal atoms replace several carbon atoms in C_{60}, the number of isomers increases significantly. For example, there are 43 distinct isomers for $C_{57}Pt_2$. DFT studies are underway on $C_{57}Pt_2$ and $C_{56}Pt_2$, and these results will be published elsewhere.

(14) Chen, Z.; Reuther, U.; Hirsch, A.; Thiel, W. *J. Phys. Chem. A* **2001**, *105*, 8105.

(15) Hirsch, A.; Nuber, B. *Acc. Chem. Res*.**1999**, *32*, 795. Chen, Z.; Ma, K.; Chen, L.; Zhao, H.; Pan, Y.; Zhao, X.; Tang, A.; Feng, J. *J. Mol. Struct.: THEOCHEM* **1998**, *452*, 219. Chen, Z.; Zhao, X.; Tang, A. *J. Phys. Chem. A* **1999**, *103*, 10961.

(16) Changgeng, D.; Jinlong, Y.; Xiangyuan, C. *J. Chem. Phys.* **1999**, *111*, 8481.

(17) The Mulliken charges given in this work are slightly different from those reported in ref 6 because the basis sets that were used were different.

(18) Yang, S. H.; Pettiette, C. L.; Concienciao, J.; Cheshnowsky, O.; Smalley, R. E. *Chem. Phys. Lett.* **1991**, *139*, 233.

(19) Lichtenberger, D. L.; Nebesny, K. W.; Ray, C. D.; Huffman, D. R.; Lamb, L. D. *Chem. Phys. Lett.* **1991**, *176*, 203.

(20) Lu, J.; Luo, Y.; Huang, Y.; Zhang, X.; Zhao, X. *Solid State Commun.* **2001**, *118*, 309.

(21) Restivo, R. J.; Ferguson, G.; Kelly, T. L.; Senoff, C. V. *J. Organomet. Chem*. **1975**, *90*, 101. Koster, R.; Seidel, G.; Kruger, C.; Muller, G.; Jiang, A.; Boese R. *Chem. Ber.* **1989**, *122*, 2075. Lundquist, E. G.; Folting, K.; Huffman, J. C.; Caulton, K. G. *Organometallics* **1990**, *9*, 2254. Wakefield, J. B.; Stryker, J. M. *Organometallics* **1990**, *9*, 2428. Einstein, F. W. B.; Yan, X.; Sutton, D. *Chem. Commun.* **1990**, 1466. Lundquist, E. G.; Folting, K.; Streib, W. E.; Huffman, J. C.; Eisenstein, O.; Caulton, K. G. *J. Am. Chem. Soc.* **1990**, *112*, 855. Bell, T. W.; Helliwell, M.; Partridge, M. G.; Perutz, R. N. *Organometallics* **1992**, *11*, 1911. Burger, P.; Bergman, R. G. *J. Am. Chem. Soc.* **1993**, *115*, 10462. Huffer, S.; Wieser, M.; Polborn, K.; Beck, W. *J. Organomet. Chem.* **1994**, *481*, 45. Batchelor, R. J.; Einstein, F. W. B.; Lowe, N. D.; Palm, B. A.; Yan, X.; Sutton, D. *Organometallics* **1994**, *13*, 2041. Cleary, B. P.; Eisenberg, R. *J. Am. Chem. Soc.* **1995**, *117*, 3510. Aizenberg, M.; Milstein, D.; Tulip, T. H. *Organometallics* **1996**, *15*, 4093. Alvarado, Y.; Boutry, O.; Gutierrez, E.; Monge, A.; Nicasio, M. C.; Poveda, M. L.; Perez, P. J. Ruiz, C.; Bianchini, C.; Carmona, E. *Chem.—Eur. J.* **1997**, *3*, 860. Antwi-Nsiah, F. H.; Torkelson, J. R.; Cowie, M. *Inorg. Chim. Acta* **1997**, *259*, 213. Gutierrez-Puebla, E.; Monge, A.; Nicasio, M. C.; Perez, P. J.; Poveda, M. I.; Rey, L.; Ruiz, C.; Carmona, E. *Inorg. Chem.* **1998**, *37*, 4538. Slugove, C.; Mereiter, K.; Trofimenko, S.; Carmona, E. *Chem. Commun.* **2000**, 121. Wiley, J. S.; Oldham, W. J., Jr.; Heinekey, D. M. *Organometallics* **2000**, *19*, 1670.

(22) Morokuma, K. *J. Chem. Phys.* **1971**, *55*, 1236. Kitaura, K.; Morokuma, K. *Int. J. Quantum. Chem.* **1976**, *10*, 325.

(23) Ziegler, T.; Rauk, A. *Theor. Chim. Acta* **1977**, *46*, 1. Ziegler, T.; Rauk, A. *Inorg. Chem.* **1979**, *18*, 1558.

(24) Campanera, J. M.; Bo, C.; Olmstead, M. M.; Balch, A. L.; Poblet, J. M. *J. Phys. Chem. A* **2002**, *106*, 12356.

(25) Nunzi, F.; Sgamelloti, A.; Re, N.; Floriani, C. *Organometallics* **2000**, *19*, 1628.

(26) Cheng, P.-T.; Nyburg, S. C. *Can. J. Chem.* **1972**, *50*, 912. Burns, C. J.; Andersen, R. A. *J. Am. Chem. Soc.* **1987**, *109*, 915. Clark, H. C.; Ferguson, G.; Hampden-Smith, M. J.; Kaitner, B.; Ruegger, H. *Polyhedron* **1988**, *7*, 1349. Camalli, M.; Caruso, F.; Chaloupka, S.; Leber, E. M.; Rimml, H.; Venanzi, L. M. *Helv. Chim. Acta* **1990**, *73*, 2263. Mole, L.; Spencer, J. L.; Carr, N.; Orpen, A. G. *Organometallics* **1991**, *10*, 49. Fulwood, R.; Parker, D.; Ferguson, G.; Kaltner, B. *J. Organomet. Chem.* **1991**, *419*, 269. Baker, M. J.; Harrison, K. N.; Orpen, A. G.; Pringle, P. G.; Shaw, G. *J. Chem. Soc., Dalton Trans.* **1992**, 2607.

(27) Dedieu, A *Chem. Rev.* **2000**, *100*, 543.

(28) Frenking, G.; Frölich, N. *Chem. Rev.* **2000**, *100*, 717.

(29) *ADF 2000.01*. Department of Theoretical Chemistry, Vrije Universiteit: Amsterdam. Baerends, E. J.; Ellis, D. E.; Ros, P. *Chem. Phys.* **1973**, *2*, 41. Versluis, L.; Ziegler, T. *J. Chem. Phys.* **1988**, *88*, 322. Te Velde, G.; Baerends, E. J. *J. Comput. Phys.* **1992**, *99*, 84. Fonseca Guerra, C.; Snijders, J. G.; Te Velde, G.; Baerends, E. J. *Theor. Chem. Acc.* **1998**, *99*, 391.

(30) Vosko, S. H.; Wilk, L.; Nusair, M. *Can. J. Phys.* **1980**, *58*, 1200.

(31) Becke, A. D. *J. Chem. Phys.* **1986**, 84, 4524. Becke, A. D. *Phys. Rev. A* **1988**, *38*, 3098.

(32) Perdew, J. P. *Phys. Rev.* **1986**, *84*, 4524. Perdew, J. P. *Phys. Rev. A* **1986**, *34*, 7406.

(33) Snijders, J. G.; Baerends, E. J.; Vernooijs, P. *At. Nucl. Data Tables* **1982**, *26*, 483. Vernooijs, P.; Snijders, J. G.; Baerends, E. J. *Slater Type Basis Functions for the Whole Periodic System*; Internal Report; Free University of Amsterdam: Amsterdam, The Netherlands, 1981.